Journal of Statistical Physics, Vol. 43, Nos. 5/6, 1986

Quantum Simulations of Aqueous Systems

Peter J. Rossky, Jürgen Schnitker,[1,2] and Robert A. Kuharski[1,3]

Discretized path-integral simulation methods have been applied to the determination of structure in two quantum mechanical aqueous systems. The first of these applications is the determination of the consequences of quantizing the rigid-body degrees of freedom of the water molecules in the many-particle pure room temperature liquid. The results provide a quantitative estimate of the significance of approximating such a system as classical and also of the size of isotope effects on the liquid structure. These features are found to have a close analogue in the structural response of the fluid to temperature. Second, we consider the structure of a hydrated excess electron. Here we treat the water classically but treat the highly quantum mechanical electron via a path-integral description, introducing a local electron–water pseudopotential for the interaction. The excess electron density and solvent distribution are examined and shown to exhibit strong structural similarities to ionic solvation. However, it is found that the electronic density fluctuates sufficiently in size and shape as to nearly erase distinct features in the electron–solvent radial correlations. For both of the aqueous systems considered, comparison of results following from the simulations with experimentally accessible direct structural measures yields satisfactory agreement.

KEY WORDS: Aqueous solutions; isotope effects; hydrated electron; water; computer simulation; path integrals.

1. INTRODUCTION

Classical computer simulation has become a powerful and widely used tool for the elucidation of the molecular level behavior of water and aqueous solutions. Nevertheless, it is clear that quantum mechanical effects are an

[1] Department of Chemistry, The University of Texas at Austin, Austin, Texas 78712.
[2] Present address: Institut für Physikalische Chemie, RWTH, Templergraben 59, 5100 Aachen, West Germany.
[3] Present address: Department of Chemistry, University of Pennsylvania, Philadelphia, Pennsylvania 19104.

0022-4715/86/0600-0949$05.00/0

essential element for certain phenomena. The two examples which we discuss here include both bulk solvent properties and solution structure.

For the bulk solvent, we consider isotopic substitution effects on liquid structure. In the absence of quantum effects, H_2O and D_2O would behave identically. However, the bulk thermodynamic properties of these fluids manifest significant differences.[1] These differences are consistent with a differential in average intermolecular interaction energy that favors pairs of D_2O molecules, as compared to H_2O pairs. Correspondingly, such quantities as the melting point and temperature of maximum density are higher by several degrees for liquid D_2O than for H_2O.

The source of the dominant contributions to quantum behavior can be anticipated. Liquid water, under the usual ambient conditions, is characterized by a space-filling network of relatively strong and directional intermolecular hydrogen bonds that produce a structure that retains a resemblance to ice.[2] That is, the molecular environment of each molecule favors a tetrahedral disposition of near-neighbor molecules, with the lowest energy configuration associated with one solvent proton lying along the line joining each pair of neighboring water oxygen atoms. Thermal agitation of this structure produces distortions and corresponding intermolecular vibrational motions. Due to the low moments of inertia of water, the highest frequency motions of this type (and hence the most quantum mechanical) are hindered rotational motions, or librations, which distort the linearity of the hydrogen bonds.[2] From either classical simulations[3] or experimental spectra,[2] one can see that such motions cover a very broad range of frequencies which for H_2O is centered at around $\omega \cong 600\,\mathrm{cm}^{-1}$ and for D_2O is closer to $400\,\mathrm{cm}^{-1}$. Hence, for a typical librational degree of freedom at 25°C, $\beta\hbar\omega \sim 2$ where β is the inverse of the product of Boltzmann's constant and the temperature and $2\pi\hbar$ is Planck's constant. Typical hindered translational motions occur at much lower frequencies and are, further, not very sensitive to isotopic substitution.

The goal of the present pure water studies[4] was to provide a quantitative estimate of the structural ramifications of quantization of the intermolecular degrees of freedom and the corresponding zero-point amplitudes that are present. Such an emphasis appears to ignore the highly quantum mechanical internal vibrations of the molecules. However, such vibrations are of a sufficiently high frequency and sufficiently small amplitude that to a good approximation one can employ a rigid-body description that implicitly accounts for averaging over these internal degrees of freedom.[5] Estimates of the structural effect produced by including such vibrations can be made,[6] but we will not discuss these here.

While the bulk solvent properties represent a case with many moderately quantum mechanical degrees of freedom, the alternative

extreme is that of a single highly quantum mechanical solute in aqueous solution. The example we consider here is that of an excess electron solvated in water. Such hydrated electrons have been the object of a great deal of experimental and theoretical analysis,[7] but direct structural observation has been quite limited.[8] Hence, our primary goal in the study of this system was to characterize this structure at a level comparable to that now available for atomic ions in water.[9,10]

As in the case of pure water, the origin of the basic phenomenon is clear.[7] The electron is localized in the liquid by a combination of effective repulsive interactions with the solvent (resulting from the orthogonality requirements between the molecular and excess electronic wavefunctions) and attractive, primarily electrostatic, solvent–electron terms. The electronic and solvent distributions are then primarily determined by a balance between the sum of solvent–electron and solvent–solvent interaction energies, and the large electronic kinetic energy produced by the confinement of the electron to a relatively small volume. The situation here is to be contrasted to the purely nonpolar solvent case in which localization arises solely due to the repulsive interactions of the electron with a disordered array of solvent particles.

With this background on the problems to be discussed here, we outline in the next section some elements of the models and methods used to carry out the structural studies. We use a discretized path integral representation of the quantum degrees of freedom[11–15] and evaluate equilibrium thermal distributions and related properties via computer simulation. This approach has already been demonstrated to be a productive route for the study of important chemical systems.[4,12–15] Section 3 presents representative results for the pure water studies including appropriate comparison to experimental scattering data, and Section 4 includes results on hydrated electron structure. The conclusions are presented in the final section.

2. MODELS AND METHODS

As indicated above, the models used to describe liquid water are rigid-body models. They have the now-standard form consisting of a spherical short-ranged Lennard–Jones interaction and a set of embedded partial electrostatic charges arranged on the nuclear framework.[16–18] For the studies of pure water, we have used the four-point charge ST2 model,[16] which places two partial positive charges at the proton positions and two negative charges in the locations characteristic of the positions of lone pair orbitals. The hydrated electron studies have employed the computationally more efficient SPC water model[18] to describe water–water interactions; here the total counterbalancing negative charge is localized on the single oxygen

site. Both models provide reasonable descriptions of pure water structure around room temperature, although the former is somewhat more thoroughly characterized.

To study electron hydration, it was necessary to develop an interaction potential of the water with the excess electron. We use a pseudopotential constructed in analogy to those in studies of electron–molecule scattering[19,20] and of the solid state.[21] The details of the potential will be published elsewhere as part of a complete report of this work.[22] Basically, the pseudopotential is based on the interaction of an electron with a water molecule, which is assumed to be fixed in the ground state electronic structure of the isolated molecule.

The interaction potential includes three contributions. The first is a purely electrostatic term which is taken to be that produced by the charge distribution of the SPC water model. This part of the potential is in reasonable accord with that calculated directly from an ab initio molecular wavefunction, except quite close to the nuclei.

The second term is a spherically symmetric polarization term, referred to the oxygen nucleus, taken from electron–molecule scattering technology. It is of the form

$$(\alpha_0/2r^4)\{1-\exp[(-r/r_0)^6]\}$$

where α_0 is the isotropic part of the molecular polarizability and r_0 is a cutoff parameter. For r_0, we use the sum of the OH bond length and the Bohr radius.

The third and most subtle term is an effective, repulsive, potential included to account for the requirements of orthogonality between the one-electron wavefunction describing the excess electron and those describing the water molecular wavefunction. We use a pseudopotential approach from solid-state physics,[21] analogous to that used some time ago to describe the electron–helium interaction.[20] Under reasonable assumptions of smoothness of the excess electron wavefunction, one can approximate this core term in a local form, in close analogy to the Slater-type local exchange approximations.[23] The final form of this part of the potential is evaluated with the s-type basis functions of a double-ζ multicenter ab initio molecular wavefunction. The repulsive core potential used consists of nine exponential terms, two centered at each hydrogen nucleus and five centered at the oxygen nucleus. Exchange terms were estimated in a local density approximation and found to be quite small compared to other uncertainties in the potential; such effects are therefore omitted.

The final potential used can be expressed as a sum of spherically symmetric terms referred to the water nuclei. The total potential is shown in

Fig. 1 as a contour plot in the water molecular plane. The general features are not surprising. It is seen that the potential exhibits minima at bond-oriented positions with an optimal attractive potential of about -35 kcal/mol (~ -1.5 eV).

To employ these potentials in the structural studies of interest here, we use discretized path-integral simulations.[4,11–15] Due to the limitations of space, we do not describe these in detail here. Detailed descriptions are available in the literature.[4,11,12,14]

The quantity of interest is the thermal distribution of electron and/or solvent positions which follows from the Hamiltonian. It has been shown[11,12] that for this case, the distribution is equivalent to the results obtained for a completely *classical* system in which the quantum particle is replaced, in the simulation, by a cyclic chain polymer consisting of P(pseudo)particles, each connected by a pair potential to its two nearest neighbors and interacting with the other particles via the potentials described above, but reduced by a multiplicative factor of P^{-1}. A simulation of this classical system provides the desired spatial distributions

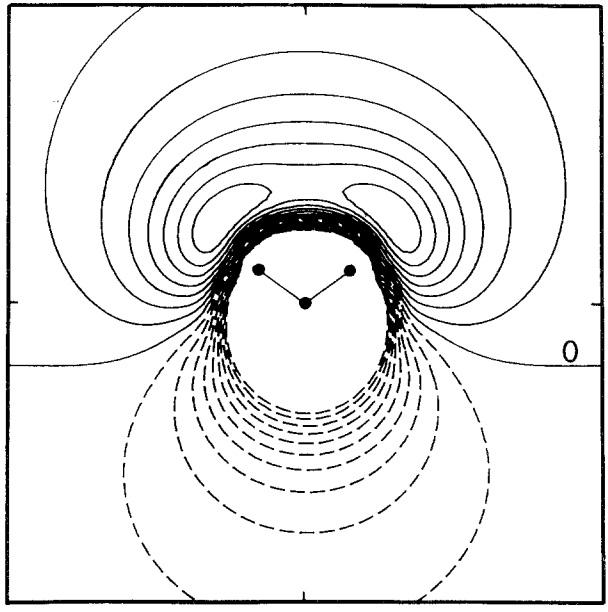

Fig. 1. Electron–water pseudopotential in the solvent molecular plane; the solvent nuclear framework is indicated, with the oxygen at the center of the 10×10 Å region shown. The contours are separated by 20 kJ/mol, starting from zero, with positive potential indicated by dashed lines and negative by solid lines. The zero potential line is labeled.

if one interprets the polymer pseudoparticle distribution as the thermal quantum density, i.e., the spatial diagonal elements of the density matrix.

For the hydrated electron studies, we have treated the solvent *purely classically*, so that only the electron is represented by such a polymer. In this case the intrapolymer pair potential is simply harmonic.[11,14] We have considered results obtained using $P = 24$, 200, and 1000, but describe here only the $P = 1000$ results, which are the most accurate. We only note here that the results for $P = 1000$ differ dramatically from those with $P = 24$ and noticeably, but not qualitatively, from those obtained with $P = 200$.[22] We believe that $P = 1000$ provides a converged result in this respect, but we have not carried out further intermediate P simulations to prove this.

For pure water, each molecule in the liquid is represented by such a polymer, with each point on the polymer including both center of mass and orientational degrees of freedom. The intrapolymer potential is harmonic for the center of mass positions but for the orientations is based on a general short-time approximation for the free rotor propagator for an asymmetric rotor. This propagator, developed for this study, is described in detail elsewhere.[4] Fortunately, for this only moderately quantum mechanical system, a rather small P is adequate. Based on the structural predictions obtained for water dimer calculations, $P = 3$ was judged adequate for the structural studies.[4]

All simulations are carried out for systems at 25°C with interactions computed in the minimum image prescription. For pure water, we have used the standard cubic periodic boundary conditions and systems containing 125 water molecules at a number density equivalent to 1 g/cc for H_2O. We have considered the liquids only at fixed number density, so that the structural effects due to quantization alone will not be clouded by those resulting from the density changes that would also follow if the structures were studied at constant pressure. The configurations were generated using an essentially standard Metropolis Monte Carlo algorithm, with separate displacement, first, for the relative positions of the P "pseudomolecules" belonging to the same polymer and, second, for the absolute center of mass position and orientation of the polymer as a whole.[4]

The hydrated electron simulations employed truncated octahedral boundary conditions,[24] which provides an efficient approach for a given number of solvent molecules and an essentially spherical solute. The simulations include 300 water molecules. Solvent–electron interactions use the electronic center-of-mass to determine the minimum image. Further, in this case, we have used molecular dynamics to sample solute and solvent configurations. We have chosen an effective mass for each electron polymer point that provides good overlap of the observed polymer dynamical frequencies and the solvent translational frequency spectrum.[22]

3. PURE WATER STRUCTURE

In this section we describe selected results pertaining to quantum effects on the structure of pure water at 25°C. We consider H_2O, D_2O, and classical systems. The latter may be viewed, for comparative purposes, as the large mass limit of the H_2O system.

In the introduction we emphasized the significance of the zero point amplitude of hindered rotational degrees of freedom, so it is reasonable to examine first the degree of nonlinearity of hydrogen bonds.

In Fig. 2, we show distributions of the cosines of the O---H–O angles for neighboring pairs of water molecules (with oxygen atoms separated by no more than 3.5 Å). Here, linearity corresponds to cos $\theta = -1$. In these calculations, only the single hydrogen atom (among the four in the molecular pair) which is closest to the $\mathbf{r}_{OO}$ vector is included. The results show that the hydrogen bonds are indeed more linear in D_2O than in H_2O, and, correspondingly, the classical liquid has the most linear hydrogen bonds of the three cases. The progression in the width of this distribution as one proceeds toward the classical thermal distribution is completely consistent with a decreasing zero-point amplitude.

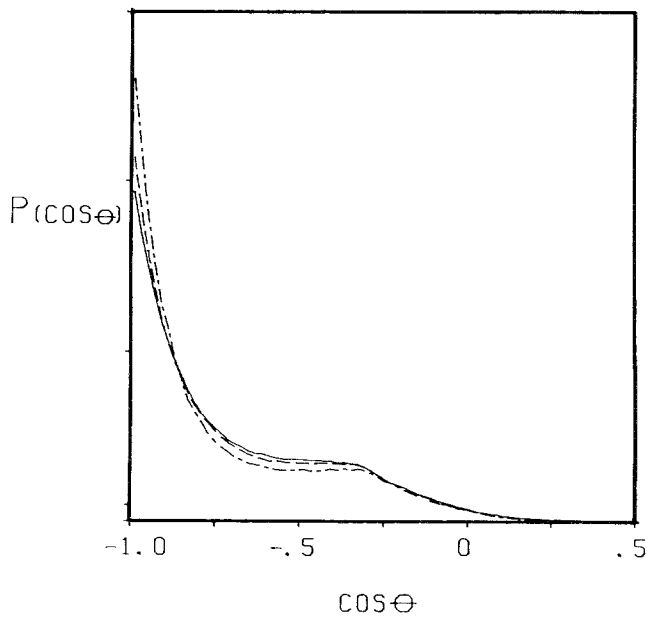

Fig. 2. Distribution of the cosines of the O---H–O angles for near-neighbor water molecules. Of the four possible hydrogen atoms for each molecular pair, only the hydrogen closest to the O–O line is included. Classical (– –), H_2O (——), D_2O(– –).

The immediate ramification of such distortions is the weakening of typical pair interactions among molecular neighbors as the quantum amplitude increases. To examine this, we have examined the distribution of pair-interaction energies found in the various isotopic liquids.

In Fig. 3 we show distributions of molecular pair-interaction energies for the three fluids. In Fig. 3a, all pairs (within the system boundary) are included, while in Fig. 3b, only near-neighbor pairs (oxygen atoms separated by no more than 3.5Å) are included. The distributions clearly show that the inclusion of quantum effects results in a shift to more positive interactions between water molecules. We note that in both distributions the D_2O curve is noticeably closer to H_2O than to classical, a result evident in other quantities as well.

Readers familiar with classical simulation results for water[16,25] will notice a strong similarity between the trends in Fig. 3 associated with increasing quantum librational amplitude and those of increasing temperature for the fluid. This analogy is not surprising, in general, since increasing temperature should also produce increased librational amplitudes. We will return below to this analogy in order to quantify the size of such quantum effects on the more useful scale of temperature.

We next turn to intermolecular radial correlations and focus in particular on the correlation between the molecular centers at the oxygen

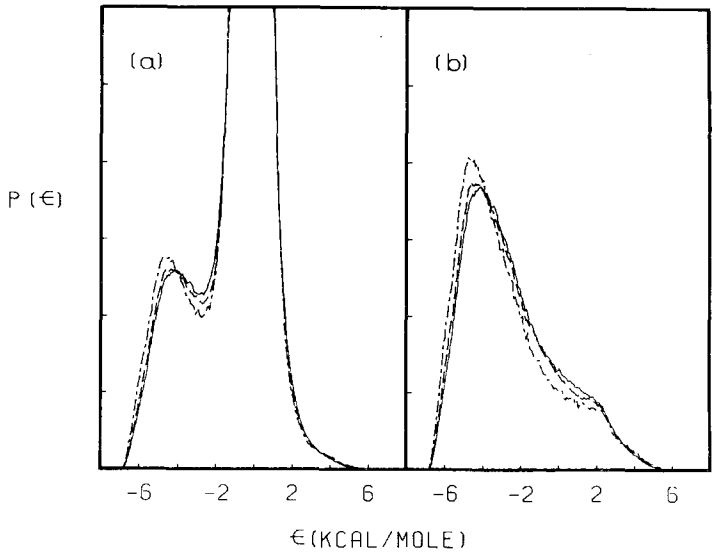

Fig. 3. Normalized distributions of pair-interaction energies for water molecules. In (a) all molecular pairs within the system boundary are included; in (b) only near-neighbor pairs are included. Classical (— –), H_2O (——), D_2O(– –).

atoms. In Fig. 4, we show the relative probabilities $g_{OO}(r)$ for the three liquids. These distributions show the trend observed in all the results, namely that the classical liquid is the most "structured" and H_2O is the least "structured." In general, the maxima decrease, the minima increase, and most importantly, the extrema occur at larger distances as the systems become more quantum mechanical. (For D_2O, the second peak in g_{OO} appears to be slightly higher than that for the classical result over a narrow range, but judging by the obvious irregularities and estimates of error bars, this is almost certainly statistical error.) The behavior observed for $g_{OO}(r)$ is also reminiscent of the changes in water structure as the temperature is raised.[16,25,26]

The second nearest-neighbor peak at about 4.8Å occurs at a distance characteristic of tetrahedral molecular coordination. The shift in the relative position of the nearest-neighbor peak at about 2.8Å, and this second-neighbor peak with increasing quantum character, is then indicative of a striking weakening in the directionality of the intermolecular interactions. This shift also provides an experimentally accessible test of the results obtained in the simulation. This is true because such a shift in relative peak positions would be reflected in associated shifts in the X ray scattering intensity pattern, the X ray source being primarily sensitive to the electron

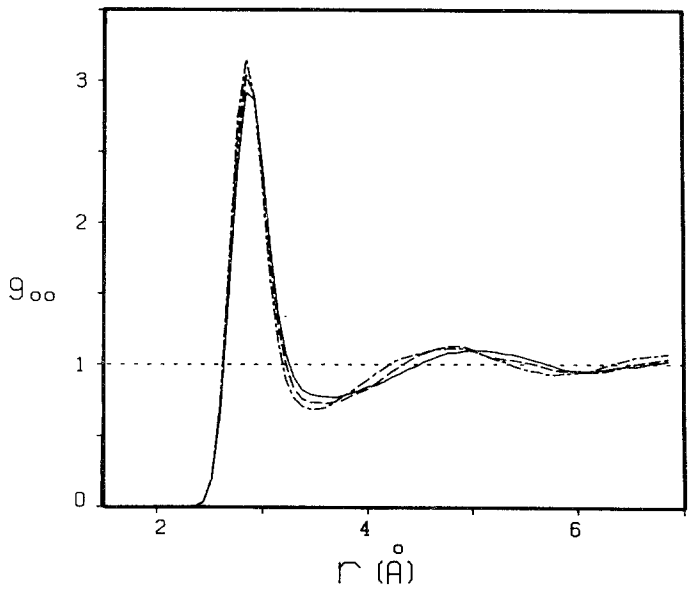

Fig. 4. Atom–atom radial distribution functions for O–O atom pairs in liquid water. Classical (— –), H_2O (——), D_2O (– –).

density associated with the oxygen. Correspondingly, the difference between the scattering pattern from H_2O and D_2O should manifest the pattern characteristic of two asynchronous oscillations.

Recent X ray diffraction studies on H_2O[27] and D_2O[28] are used to look for evidence of these quantum effects. In both instances, the data have been reported in terms of the so-called molecular center structure factors $H_m(k)$, and we will use these for comparison. The H_2O data is for 25°C. The structure factor for D_2O at 11.2°C has been given along with several isochoric temperature differentials (ITD). We estimate the D_2O structure factor at 25°C (and a density nearly identical to H_2O at 25°C) from the one given by adding a first-order correction based on the ITD reported for a 23.3°C temperature change, which is expected to be a good approximation.[29] For comparison, we calculate theoretical molecular center structure factors for H_2O and D_2O from the simulated partial structure factors.[4,29]

We subtract the D_2O structure factors from those of H_2O for both the experimental and theoretical results, and in Fig. 5 we show these differences. The results are very encouraging. The theoretical results below 1 $Å^{-1}$ are not reliable due to truncation effects, but beyond this region the curves exhibit the same qualitative behavior and have comparable magnitudes. It should be noted that although the differences we are comparing are small, the stated precision of the experiments indicates that they are significant.

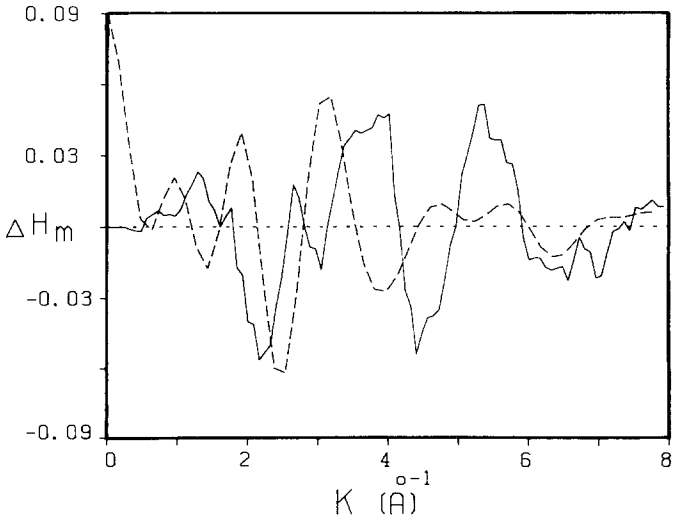

Fig. 5. Differences between the molecular center structure factors of H_2O and D_2O. Prediction based on X ray diffraction results (——), theoretical results (– –).

It is of substantial interest to obtain a familiar measure by which to assess the significance of quantum effects. As indicated above, a useful measure is the temperature scale. In particular, we can ask what temperature rise in liquid water produces structural changes comparable to those induced by quantization of H_2O. Examination of classical simulation results[16,25] for water shows[4] that both the amplitude of correlation functions and the propensity for hydrogen bonding change upon quantization by amounts comparable to a temperature increase of 40° to 50°C.

We can also make a direct structural comparison of our results with the effects of temperature as observed experimentally via X ray diffraction. We employ the heavy water results of Bosio, Chen, and Teixeira[28] who report the changes in the molecular center radial distribution function g_m for temperature differences of 8.4, 23.3, and 51°C. We compare to the calculated molecular center correlation functions for our classical and quantum treatments of H_2O and obtain the results shown in Fig. 6; the experimental result for a 51°C temperature change and the H_2O, quantum minus classical, result are shown. The general agreement between these results is excellent, indicating that the analogy between quantization effects and temperature influence is sound. Hence, the use of temperature differences to conceptualize quantum effects in this case is clearly a productive route.

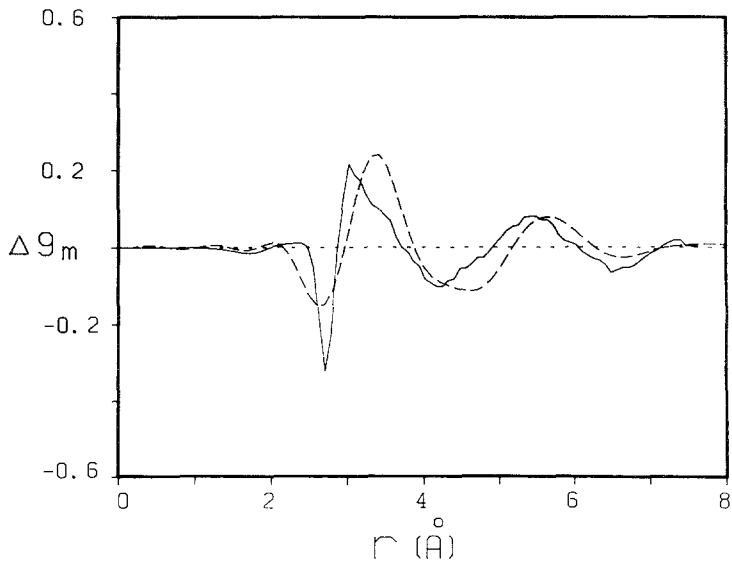

Fig. 6. Changes in the molecular center distribution function. X ray results for a 51° rise in temperature from Ref. 28 (––); differences between quantum and classical results at 25°C (——).

4. EXCESS ELECTRON SOLVATION

In this section, we present some illustrative results obtained from the path integral simulation of an excess electron in bulk *(classical)* liquid water. Here we emphasize results for the solvent orientational and radial distribution with respect to the quantum electron.

We first consider briefly the structure of the electron *per se*. One of the important features of path-integral simulations is the ability to readily visualize the spatial distribution of the quantum particle by displaying representative paths which contribute to the spatial density. A typical electron path is shown in Fig. 7. Here we have displayed the 1000 points (P) of the electron path sampled in this case, each connected to its neighbors in the "polymer" by a straight line. The edges of the truncated octahedral boundary containing the centers of the 300 solvent molecules is indicated. The electron is clearly localized and roughly spherical, with a radius of

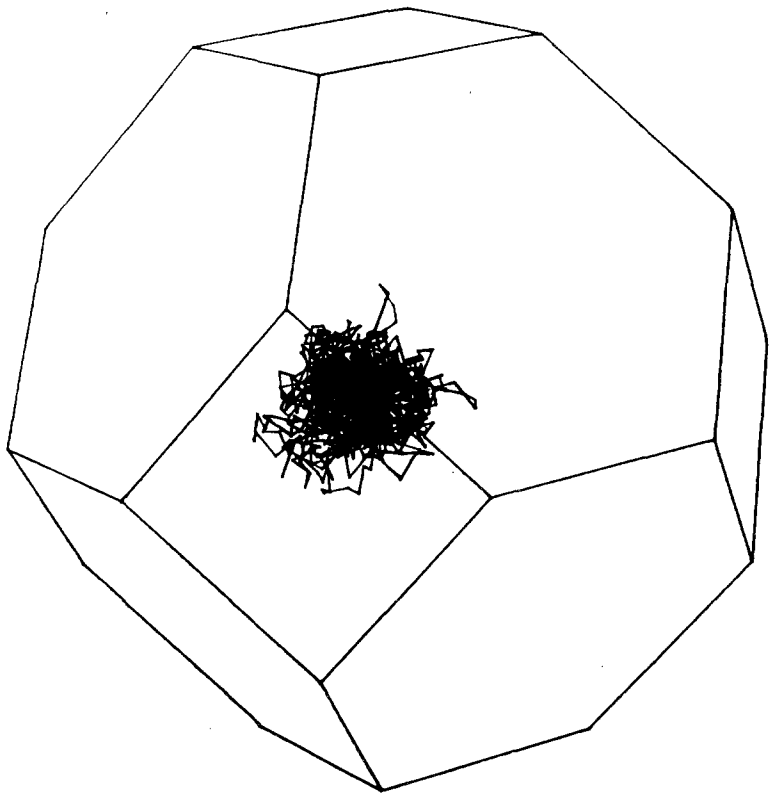

Fig. 7. Representative electron path for $P = 1000$. The boundary containing the 300 water molecules is also indicated.

about 2.5Å (see below), in general agreement with earlier estimates.[7] However, the electronic distribution clearly manifests irregularities and extended regions at its surface.

The solvent orientational structure can be analyzed in much the same way as for ordinary atomic solutes, as shown in Fig. 8. There, for the first solvation shell, we show the distribution of solvent dipole directions (solid lines) and OH bond directions (dashed lines) with respect to the electron position, plotted as a function of the cosine of the angle formed by this vec-

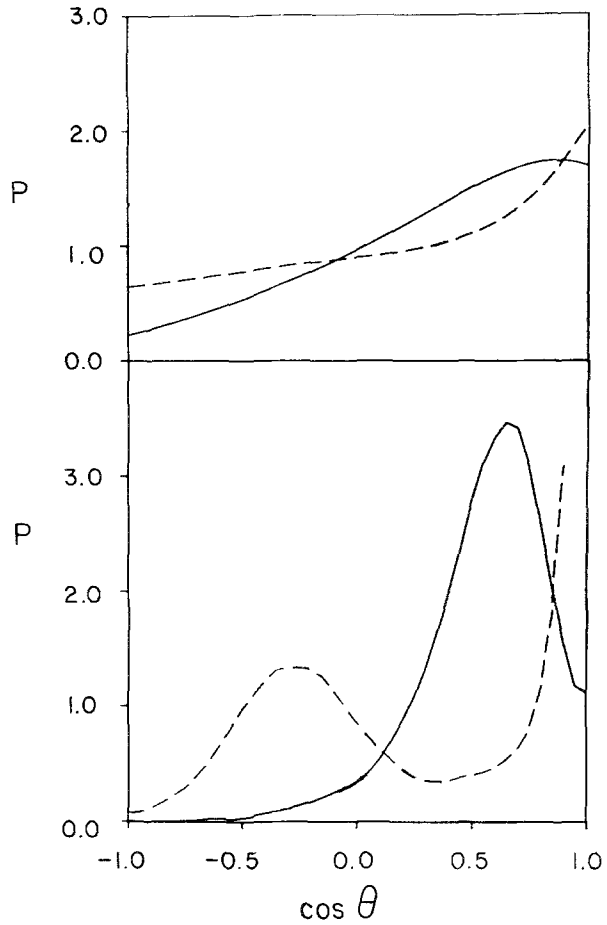

Fig. 8. Relative distribution of solvation shell solvent OH bond (--) and dipole (——) directions with respect to the solvent oxygen–electron position vector; $\cos\theta = -1$, at the left, corresponds to a solvent direction which points away from the electron. The upper curves include all electron positions on the path; the lower set of curves refer to the electronic center of mass.

tor with respect to the oxygen to electron vector; the distribution is normalized so that unity is the random orientational value. The upper frame includes all electronic positions on the path and hence is relatively diffuse. The lower frame corresponds to an electronic reference point at the center of mass of the electronic distribution, and corresponds to the view familiar from analysis of atomic ion solvation.[9,10]

As is clear from the figure, the solvent is bond-oriented as it is around a negative atomic ion.[9] This structure is perhaps predictable based on the potential shown in Fig. 1, but contrasts with the dipolar orientation frequently assumed in simplified theoretical treatments.[7] Except for a somewhat increased breadth in the peaks, the distribution is, in fact, exactly that which has been observed in earlier negative ion solvation studies.

The radial distribution of solvent is shown in Fig. 9. As in Fig. 8, the upper set of curves corresponds to all points in the electronic distribution while the lower curve describes the distribution with respect to the electronic center of mass; the dashed line is the solvent hydrogen distribution and the solid line is that of the oxygen. As above, we focus on the lower set of curves.

For $P = 1000$, the radial correlations are clearly quite different in first appearance from ion-like behavior. For a hydrated ion, the radial correlations manifest sharply defined solvation layer structure.[9,10] For example, for a typical model of Cl^- in aqueous solution,[10] one finds that the chloride–oxygen correlation function exhibits a distinct first layer peak at about 3.3Å with a peak height of about 2.8. The first ion–hydrogen peak occurs about 1Å closer to the ion at about 2.3Å, with a peak height of close to 2.5. The number of nearest-neighbor water molecules, or coordination number, obtained from radial integration of the distribution function is about 7.

For electron hydration, the bond orientation of the solvent is still apparent (hydrogen approaching ~ 1Å closer to the electronic center than does oxygen), but both hydrogen and oxygen peaks are strongly broadened. Nevertheless, the electron is solvent-coordinated in an ionic-like manner; the coordination number obtained from integration of the oxygen radial correlation function shown at the bottom in Fig. 9 is between 5 and 6, depending on the choice of radial position used to determine the radius of the first solvation shell.

Considering the well-defined orientational correlations found and the reasonable, and relatively small, coordination number observed, it is reasonable to attribute the apparent diffuse nature of the radial correlations to fluctuations in the shape and radius of the excess electron, rather than to a *lack* of structure. In fact, an examination of a sequence of paths

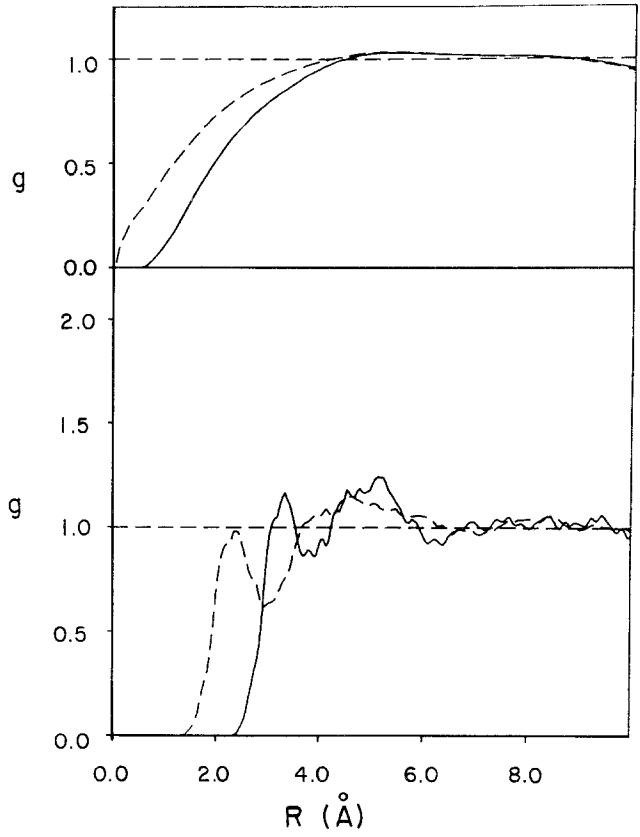

Fig. 9. Electron–solvent radial correlation functions, g_{eH} (--) and g_{eO} (——). Upper and lower sets of curves include all electron positions on the path, or only the electronic center of mass, respectively.

analogous to that shown in Fig. 7 supports this view. It is in this respect that the solution containing an excess electron differs most from that with a simple ion. The electron exhibits the solvation structure that would be expected of an ion which had the additional freedom to fluctuate in size and shape, while remaining compact and roughly spherical.

Finally, it is of interest to compare, as far as possible, the calculated structure to experimental results. While inferences have been drawn from a variety of measurements,[7] one direct structural analysis has been carried out.[8] Using electron spin echo measurements to determine a set of solvent proton populations and distances in an aqueous glass, Kevan has proposed a specific idealized structure for the hydrated electron. Keeping in mind that the glass is formed at high salt concentration, we can compare the

liquid state results described above to the experimental assessment. Kevan finds that his data are best fit by a (glassy) solvent with six nearest-neighbor protons at a distance of 2.1Å and a second set of six protons at a distance of 3.5Å from the electronic center, implying an electron–oxygen distance of 3.1Å and bond-oriented solvent.

The present results are in very good accord with these results. We find a roughly six-coordinate, bond-oriented solvent, with the nearest protons centered at 2.3Å and oxygen atoms centered at 3.3Å (see Fig. 9). Considering the difference in system composition, the limited information which can be extracted from the experiment, and the uncertainties in our present potential, the agreement in structural results is quite striking. Not surprisingly, the present results clearly show a substantial degree of dispersity in the detailed solvation structure which cannot be a priori extracted from the experimental data. It is now of substantial interest to explore the degree to which the experimental probe is sensitive to such fluctuations, so that a potentially more demanding test of the validity of the detailed theoretical results can be constructed.

5. CONCLUSIONS

Path-integral simulation methods can now provide insight into quite complex quantum chemical systems, which is presently not available via direct experimental probe. This ability is clearly expanding rapidly with emerging new techniques and new computer facilities.

From the present examples, it is clear that although both detail and insight are emerging from such new studies, many elements of aqueous system behavior and its modeling remain to be explored. For example, the sensitivity of the results described to the interaction potential employed is not yet established. The area of quantum simulations in chemical systems is still quite new, and the study of electron solvation is only a first step in a detailed understanding of such complex chemical processes as molecular ionization and electron transfer reactions in liquids. Based on the already rapid growth of this field, these more demanding cases will no doubt be accessible to comparable analysis in the near future.

ACKNOWLEDGMENTS

We thank Michael Sprik, Roger Impey, and Michael Klein for the open communication of the results of their related studies of solvated electrons prior to publication. The work reported here was supported by grants from the National Institute of General Medical Sciences and the

Robert A. Welch Foundation, and by a generous grant of computer time from Cray Research, Inc. P. J. R. is an Alfred P. Sloan Foundation Fellow, and the recipient of an NSF Presidential Young Investigator Award, a Dreyfus Foundation Teacher-Scholar Award, and an NIH Research Career Development Award from the National Cancer Institute, DHHS.

REFERENCES

1. G. Nemethy and H. A. Scheraga, *J. Chem. Phys.* **41**:680 (1964).
2. D. Eisenberg and W. Kauzmann, *The Structure and Properties of Water* (Oxford Press, London, 1969).
3. A. Rahman and F. H. Stillinger, *J. Chem. Phys.* **55**:3336 (1971).
4. R. A. Kuharski and P. J. Rossky, *J. Chem. Phys.* **82**:5164 (1985).
5. F. H. Stillinger, *Adv. Chem. Phys.* **31**:1 (1975).
6. R. A. Kuharski and P. J. Rossky, *J. Chem. Phys.* **82**:5289 (1985).
7. N. R. Kestner in *Electron-Solvent and Anion-Solvent Interactions*, L. Kevan and B. C. Webster, eds. (Elsevier, New York, 1976); D. F. Feng and L. Kevan, *Chem. Rev.* **80**:1 (1980); E. J. Hart and M. Anbar, *The Hydrated Electron* (Wiley, New York, 1970).
8. L. Kevan, *J. Phys. Chem.* **85**:1628 (1981).
9. M. Mezei and D. L. Beveridge, *J. Chem. Phys.* **74**:6902 (1981); J. Chandresekhar, D. C. Spellmeyer, and W. L. Jorgensen, *J. Am. Chem. Soc.* **106**:903 (1984).
10. R. W. Impey, P. A. Madden, and I. R. McDonald, *J. Phys. Chem.* **87**:5071 (1983).
11. R. Feynman, *Statistical Mechanics* (Benjamin, Reading, Massachusetts, 1972).
12. D. Chandler, and P. G. Wolynes, *J. Chem. Phys.* **74**:4078 (1981).
13. D. Thirumalai, R. W. Hall, and B. J. Berne, *J. Chem. Phys.* **81**:2523 (1984).
14. M. Parrinello and A. Rahman, *J. Chem. Phys.* **80**:860 (1984).
15. B. DeRaedt, M. Sprik, and M. L. Klein, *J. Chem. Phys.* **80**:5719 (1984).
16. F. H. Stillinger and A. Rahman, *J. Chem. Phys.* **60**:1545 (1974).
17. W. L. Jorgensen, J. Chandrasekhar, J. D. Madura, R. W. Impey, and M. L. Klein, *J. Chem. Phys.* **79**:926 (1983).
18. H. J. C. Berendsen, J. P. M. Postma, W. F. VanGunsteren, and J. Hermans, in *Intermolecular Forces*, B. Pullman, ed. (Reidel, Dordrecht, Holland, 1981).
19. D. G. Truhlar, K. Onda, R. A. Eades, and D. A. Dixon, *Int. J. Quant. Chem. Symp.* **13**:601 (1979).
20. J. Jortner, N. R. Kestner, S. A. Rice, and M. H. Cohen, *J. Chem. Phys.* **43**:2614 (1965).
21. V. Heine, *Solid State Phys.* **24**:1 (1970).
22. J. Schnitker and P. J. Rossky (manuscript in preparation).
23. S. Hara, *J. Phys. Soc. Japan* **22**:710 (1967).
24. W. F. VanGunsteren, H. J. C. Berendsen, F. Colonna, D. Perahia, J. P. Hollenberg, and D. Lellouch, *J. Comp. Chem.* **5**:272 (1984).
25. M. Mezei and D. L. Beveridge, *J. Chem. Phys.* **74**:62 (1981).
26. A. H. Narten, M. D. Danford, and H. A. Levy, *Discuss. Faraday Soc.* **43**:97 (1967).
27. K. Nishikaua and N. Kitagawa, *Bull. Chem. Soc. Japan* **53**:2804 (1980).
28. L. Bosio, S. Chen, and J. Teixeira, *Phys. Rev. A.* **27**:1468 (1983).
29. P. A. Egelstaff and J. H. Root, *Chem. Phys.* **76**:405 (1983).